Progress In Electromagnetics Research C, Vol. 22, 109–122, 2011

A COMPACT DUAL-BAND COUPLED-LINE BALUN WITH TAPPED OPEN-ENDED STUBS

J. Shao[1], H. Zhang[1, *], C. Chen[2], S. Tan[3], and K. J. Chen[4]

[1]Department of Electrical Engineering, University of North Texas, Denton, TX 76207, USA

[2]Department of Electronic Engineering and Information Science, University of Science and Technology of China, Hefei, Anhui 230027, P. R. China

[3]Department of Computer Science City, University of Hong Kong, Hong Kong, P. R. China

[4]Department of Electronic and Computer Engineering, Hong Kong University of Science and Technology, Clear Water Bay, Kowloon, Hong Kong, P. R. China

Abstract—This paper presents a novel structure for compact dual-band balun design. The proposed structure is based on modified Marchand (with the fourth port shorted). To achieve the desired dual-band operation, two additional open-ended stubs are added to the two balanced ports of the modified Marchand balun. Explicit design equations are then derived using even-odd mode analysis. Finally, to verify the design concept, a microstrip balun operating at 0.9/2 GHz are fabricated on Duroid RO3210 printed circuit board. Measurement results are in good agreement with the theoretical predictions.

1. INTRODUCTION

Balun is a microwave device for converting unbalanced signals to balanced one, and vice versa [1–3]. Such conversion is attractive, especially for differential-mode -RF/microwave circuits, since it will lead to improved signal timing, reduced electromagnetic interference and noise. Baluns can also be used as 180 hybrids, which further extends their applications [4]. The conventional baluns can be

Received 2 May 2011, Accepted 15 June 2011, Scheduled 20 June 2011

* Corresponding author: Hualiang Zhang (hualiang.zhang@unt.edu).

categorized into two types, namely, active and passive baluns. For active baluns, the transistors employed will consume more energy [5]. As for passive baluns, they can be classified as lumped-type and distributed-type [6–8]. The disadvantage of lumped-type balun is that it is difficult to maintain the 180° phase difference and equal magnitude response between the two signals. The distributed-type Marchand balun features low loss, uni-planar structure, and low cost [9]. Therefore, this kind of balun is attractive for practical applications.

Meanwhile, with the rapid advance in wireless communications, the designs of many passive circuits are facing new challenges including compact size, wide bandwidth and multi-band operations. For example, high data-rate wireless communication systems, such as worldwide interoperability for microwave access (WiMAX) and wireless local area network (WLAN), require wide bandwidth up to several hundred of megahertz and flexibility of operating in multiple frequency bands. Among all of these new requirements, the multi-band operation is very important. It can lead to both the size and cost reduction of the whole system.

For balun design, different topologies had been studied for size reduction [10–13] and bandwidth enhancement [14–16]. Efforts on multi-band baluns, however, are limited. Guo et al. realized a dual-band balun by replacing the uniform coupled-lines with tapered coupled-lines in a Marchand balun [17]. Another dual-band balun has been proposed using stepped impedance resonators in the coupled-line Marchand balun [18]. This structure features multiple coupled units that need careful tuning and tight control in the prototype fabrication. In [19], based on the conventional Marchand balun, a dual-band balun was achieved by attaching two open stubs. Apart from Marchand-type balun, another dual-band balun based on branch line structure has also been proposed [20, 21]. This design has a good performance and is easy to realize. However, the physical size of this structure is large.

To address this issue, in this paper, we propose and demonstrate a novel compact structure of dual-band baluns. In this structure, two open-ended stubs are connected at the balanced ports of a modified Marchand balun. By adjusting the stub impedances and coupled-line even-odd mode impedances, the desirable equal-amplitude and out-of-phase responses can be achieved at two operating frequencies. For the purpose of experimental demonstration, a microstrip balun working at 0.9/2 GHz is fabricated on printed circuit boards (PCB). The measurement results verified the design concept.

2. THEORETICAL ANALYSIS

2.1. Design Concept of Dual-Band Balun

A 3-port balun circuit can be obtained by terminating one port of a symmetrical 4-port network with arbitrary port impedances [22]. Fig. 1(a) illustrates an example of realizing 3-port baluns based on 4-port networks, where a short termination is applied at one specified port (port 4). Here, all the coupled-line sections are quarter-wavelength long.

To achieve the dual-band operation, two additional stubs are attached at the two balanced ports of the modified Marchand baluns as shown in Fig. 1(b), leading to the proposed dual-band balun. The electrical lengths of the couple line sections in this balun are θ_c, and the length of the shunted stubs is θ_s. An intuitive explanation of the design concept is that the shunted stubs introduce a transmission zero in the pass-band so that the fundamental band splits into two separate operating bands. In addition, it is found that θ_s must be an integer multiple of θ_c. The impedance of the stub and the even-odd mode impedances are functions of the input/output impedances of the balun. Detailed mathematical derivations of these parameters will be provided.

Applying the even-odd analysis method, the even- and odd-mode equivalent circuits of the proposed balun are shown in Figs. 2(a) and (b). Γ_e and Γ_o are the input reflection coefficients of the even- and odd-mode circuits, while T_e and T_o are the transmission coefficients. Γ is the reflection coefficient of port 4. The following relationships have

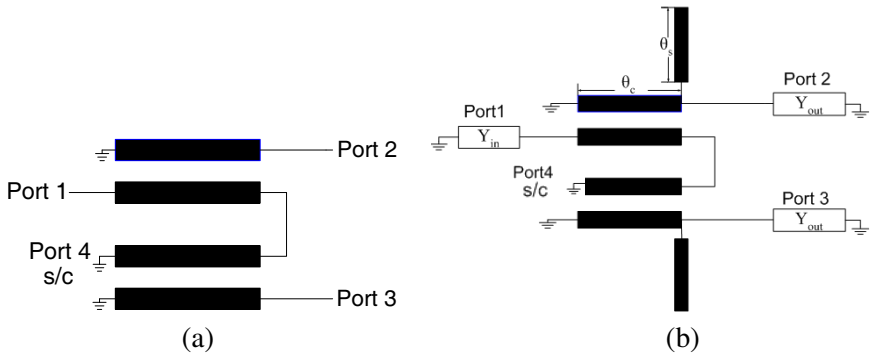

Figure 1. (a) Modified Marchand balun with a short-ended port 4. (b) General schematic of the proposed dual-band balun.

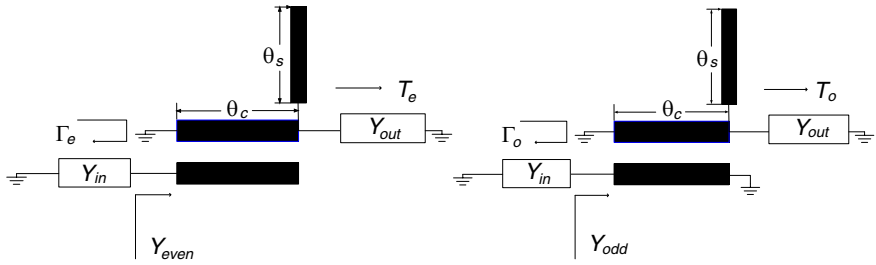

Figure 2. (a) Equivalent circuit under even-mode excitation. (b) Equivalent circuit under odd-mode excitation.

been derived for synthesizing this kind of 3-port baluns [22].

$$\frac{T_e \cdot (1 - \Gamma_o \cdot \Gamma)}{2 - \Gamma \cdot (\Gamma_e + \Gamma_o)} = 0 \tag{1a}$$

$$\frac{\Gamma_e + \Gamma_o - 2\Gamma_e \Gamma_o \Gamma}{2 - \Gamma(\Gamma_e + \Gamma_o)} = 0 \tag{1b}$$

The first Equation (1a) is to ensure that $S_{21} = -S_{31}$, while the second equation considers the matching condition at port 1 (input port), $S_{11} = 0$. These equations imply that, to achieve perfect amplitude and phase balance, the balun has to present a transmission stop for the even-mode circuit, that is $T_e = 0$. When it comes to the odd-mode circuit, the solution will vary depending on the termination of port 4 (depending on Γ). Since port 4 is grounded in our case ($\Gamma = -1$), the corresponding conditions for balun operation are:

$$\Gamma_e = 1 \quad \text{and} \quad \Gamma_o = -\frac{1}{3} \tag{2}$$

By substituting Y_{even}, Y_{odd} and $\mathrm{Y_{in}}$ (defined in Fig. 2) into (1b), more insightful conclusions are obtained [23]:

$$Y_{even} + Y_{odd} = 2Y_{in} \tag{3}$$

In our case, the even-mode circuit (Fig. 2(b)) of the proposed dual band balun structure is naturally a transmission stop network for all bands. In fact, this is one of the ten typical two-port coupled line structures discussed in [24]. Similarly, the odd-mode circuit can be analyzed. The details regarding the derivations of Y_{even} and Y_{odd} are discussed below.

First, we write the $ABCD$ matrix of the even mode circuit. Then from the $ABCD$ matrix, S_{11} can be gotten. Finally, from S_{11} we can

derive the Y_{even}. The derivation of odd mode circuit follows the same procedure. After a lengthy analysis process, the final results are as follows (note: for the ease of expression, we have listed the real and imaginary part of Y_{even} and Y_{odd} separately):

$$Y_{even}(real) = \frac{\begin{array}{l} -8a^2\cdot Y_{out}\cdot\sin^2(2\theta_c)\cdot(a^2-b^2)+32a^3\sin^2\theta_c\cdot\sin 2\theta_c\cdot Y_s\cdot\tan\theta_s\cdot Y_{out} \\ -4a^2\cdot(a^2-b^2)\sin^2(2\theta_c)\cdot Y_{out}+32a^3\cdot Y_{out}\cdot Y_s\cdot\tan\theta_s\cdot\sin^2\theta_c\cdot\sin 2\theta_c \end{array}}{\begin{array}{l} 16\cos^4\theta_c\cdot(a^2-b^2)^2-32a\cdot\cos^2\theta_c\cdot(a^2-b^2)\cdot\sin 2\theta_c\cdot Y_s\cdot\tan\theta_s \\ +16a^2\cdot\sin^2(2\theta_c)\cdot(Y_s\cdot\tan\theta_s)^2+16a^2\sin^2(2\theta_c)\cdot Y_{out}^2 \end{array}} \quad (4)$$

$$Y_{even}(imaginary) = \frac{\begin{array}{l} -4a\cdot(a^2-b^2)^2\cdot\sin 2\theta_c\cdot\cos^2\theta_c+4a^2\sin^2(2\theta_c)\cdot(a^2-b^2)\cdot Y_s\cdot\tan\theta_s \\ +8a^2\cdot(a^2-b^2)\sin^2(2\theta_c)\cdot Y_s\cdot\tan\theta_s+32a^3\cdot Y_{out}^2\cdot\sin^2\theta_c\cdot\sin 2\theta_c \end{array}}{\begin{array}{l} 16\cos^4\theta_c\cdot(a^2-b^2)^2-32a\cdot\cos^2\theta_c\cdot(a^2-b^2)\cdot\sin 2\theta_c\cdot Y_s\cdot\tan\theta_s \\ +16a^2\cdot\sin^2(2\theta_c)\cdot(Y_s\cdot\tan\theta_s)^2+16a^2\sin^2(2\theta_c)\cdot Y_{out}^2 \end{array}} \quad (5)$$

$$Y_{odd}(real) = \frac{\begin{array}{l} Y_{out}\cdot a^2\cdot\sin^2(2\theta_c)-4\sin^2\theta_c\cdot\sin 2\theta_c\cdot a\cdot Y_s\cdot\tan\theta_s-4b^2\sin^2\theta_c \\ \cdot Y_{out}+a^2\cdot Y_{out}\sin^2(2\theta_c)-4a\cdot\sin^2\theta_c\cdot\sin 2\theta_c\cdot Y_{out}\cdot Y_s\cdot\tan\theta_s \end{array}}{\begin{array}{l} \sin^2(2\theta_c)\cdot a^2-8a\cdot\sin^2\theta_c\cdot\sin 2\theta_c\cdot Y_s\cdot\tan\theta_s \\ +16(Y_s\cdot\tan\theta_s)^2\cdot\sin^4\theta_c+16\sin^4\theta_c\cdot Y_{out}^2 \end{array}} \quad (6)$$

$$Y_{odd}(imaginary) = \frac{\begin{array}{l} -ab^2\sin(2\theta_c)+a^3\sin 2\theta_c\cdot\cos^2\theta_c-2a^2\cdot\sin^2(2\theta_c)\cdot Y_s\cdot\tan\theta_s+4b^2 \\ \sin^2(2\theta_c)\cdot Y_s\cdot\tan\theta_s+4a\cdot\sin(2\theta_c)\cdot\sin^2\theta_c\cdot((Y_s\cdot\tan\theta_s)^2-Y_{out}^2) \end{array}}{\begin{array}{l} \sin^2(2\theta_c)\cdot a^2-8a\cdot\sin^2\theta_c\cdot\sin 2\theta_c\cdot Y_s\cdot\tan\theta_s \\ +16(Y_s\cdot\tan\theta_s)^2\cdot\sin^4\theta_c+16\sin^4\theta_c\cdot Y_{out}^2 \end{array}} \quad (7)$$

where $a = Y_{oe} + Y_{oo}$, $b = Y_{oo} - Y_{oe}$, Y_{oo} and Y_{oe} are the even- and odd-mode admittances of the coupled-line unit, Y_s is the admittance of the stub (with a length of θ_s as shown in Fig. 2). θ_c and θ_s are the electric length of the coupled-line sections and the shunted stubs, respectively.

Y_{odd} and Y_{even} are then derived as functions of θ_c, θ_s, Y_{in}, Y_{out} and Y_s, assuming

$$\theta_s = n \times \theta_c \quad (8)$$

where $\theta_c = 0°@(f_1 + f_2)/2$.

From the above design equations, we can predict the following proprieties of the solutions of Y_{even} and Y_{odd} versus θ_c: They are periodic and symmetrical in nature with period equating to π, since "θ_c" and "$\pi - \theta_c$" give the same expression. This is the intrinsic property of proposed structures for dual band operation.

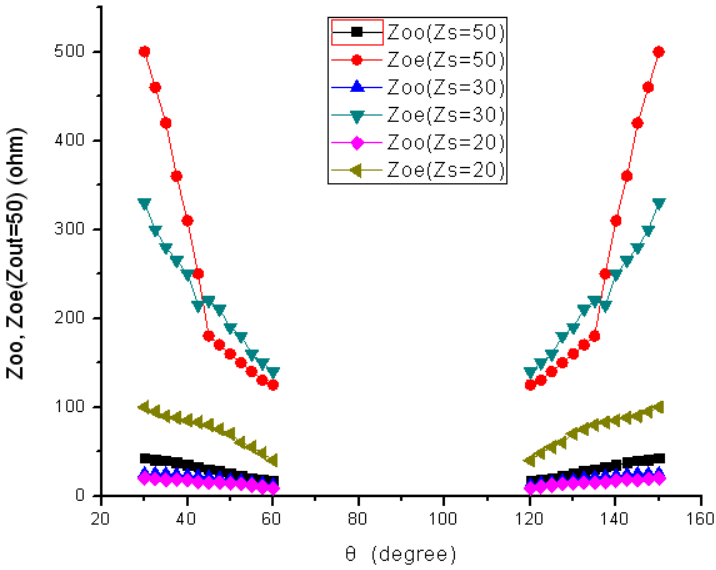

Figure 3. Design curves for determining Z_{oe}, Z_{oo} with different Z_s in 50–50 Ω system.

Applying Eqs. (1)–(8), the solutions of Z_{oe}, Z_{oo} for different terminations can be calculated (some of these results are given in Figs. 3–5). Fig. 3 shows the solutions of Z_{oe}, Z_{oo} in the 50–50 Ω system. We set $n = 1$ for the most compact design. It can be seen that the balun could be realized by the practical value of Z_{oe} and Z_{oo} with θ_c between 30° and 60° as well as 120° and 160° depending on the value of stub impedance Z_s. In general, the required values of Z_{oe} and Z_{oo} increase with increasing Z_s. For θ_c in the 30° to 60° range, Z_{oe} and Z_{oo} decrease monotonically with increasing θ_c.

Figure 4 shows the solutions in impedance transforming system (input and output port have different impedance). It is observed that, when the ratio increases, the distance between even and odd mode impedances decreases, leading to decreased coupling coefficient. This implies that higher impedance transformation ratio is easier to be implemented in practice.

2.2. Discussion for Larger n

The above discussion is based on $n = 1$ situation (n is defined in Eq. (8)), which means the stub and the couple line have the same

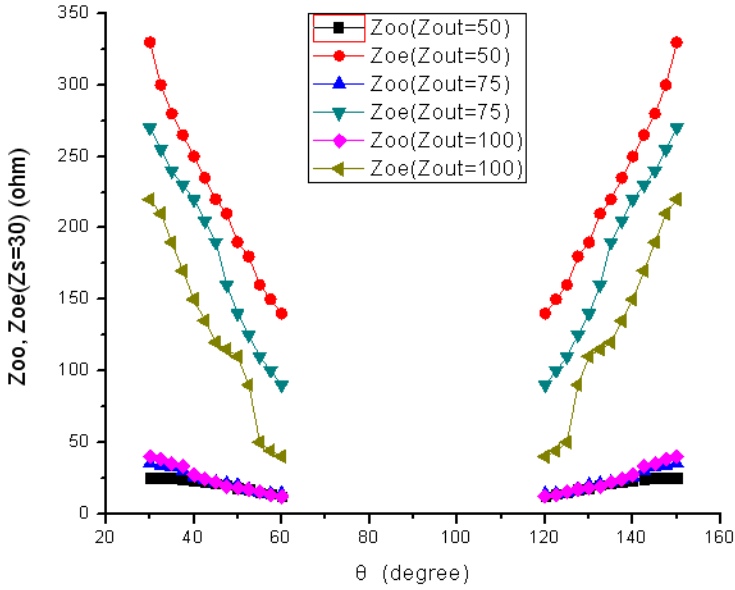

Figure 4. Design curves for determining Z_{oe}, Z_{oo} with different output impedances ($Z_{in} = Z_s = 30\,\Omega$).

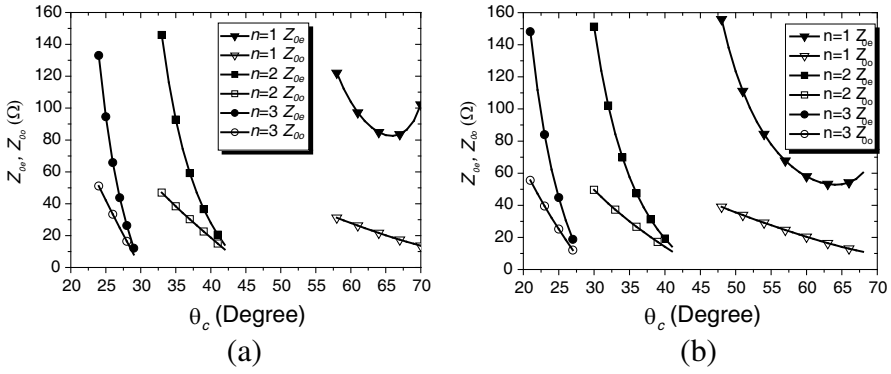

Figure 5. (a) Calculated even-odd mode impedance with different n for $Z_s = 110\,\Omega$, and (b) $Z_s = 80\,\Omega$ in 50–250 system.

length. For larger n, larger design flexibility can be achieved. Fig. 5 shows the even-odd mode impedances when n equals to 1, 2 and 3. These parameters are calculated in 50–250 system. In Fig. 5(a), the shunted stub impedance (Z_s) is $110\,\Omega$, we can see that the $n = 1$ case

only covers 57° to 70° for θ_c, the $n = 2$ case covers 33° to 43° while the $n = 3$ case covers 22° to 30°. Fig. 5(b) shows the calculated results when the stub impedance (Z_s) is 80 Ω. Compared with the results shown in Fig. 5(a), the practical frequency range changes a bit with different n. But the overall trend stays the same. These examples show clearly the influence of n on the proposed designs.

3. DESIGN PROCEDURE

The design procedure of the new dual-band balun could be summarized as the following steps:

(1) The couple line electric length is 90° at the middle frequency of two operating bands. The length of coupled line should be designed first.

(2) Due to the linear relation between frequency and electrical length or physical length, we can calculate the electrical length at lower frequency and higher frequency band as $(f_1/f) \times 90°$ and $(f_2/f) \times 90°$, respectively. According to input-output impedances of the system, we can get the different combinations of even-odd mode impedances at smaller and larger electrical length with respect to lower and higher frequency bands for different n values (Eqs. (1)–(8) are applied). The two impedances are the same due to the symmetrical property. We should choose the smallest n and appropriate stub impedance which can satisfy the design requirements and ensure that the resulting even-odd mode impedances can be realized in practical fabrication.

(3) According to n, we can compute the length of the shunted stubs. From the stub impedance and even-odd mode impedances, we can finally calculate the physical dimensions of the microstrip line and the coupled line.

Table 1 shows some typical combinations of dual operation frequencies. Since the GSM system and IEEE 802.11 standard are often used, the corresponding design parameters for them are listed in this table. The resulting dual-band baluns could be easily implemented using different fabrication techniques. The schematic-level simulation results are shown in Fig. 6.

4. PROTOTYPE FABRICATION AND MEASUREMENT

To demonstrate the feasibility of our design concept, validate the analytical results and evaluate the performance of proposed structures, a balun was fabricated for 50–250 Ω system. For this balun, it can

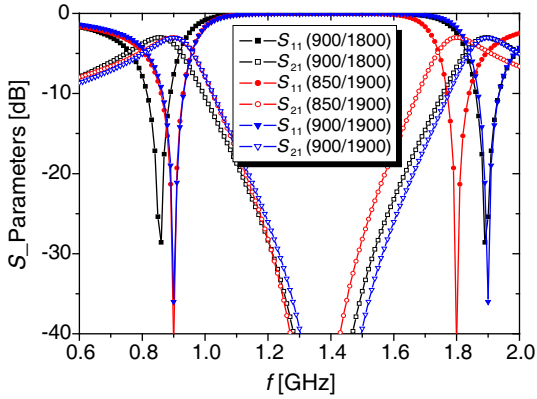

(a)

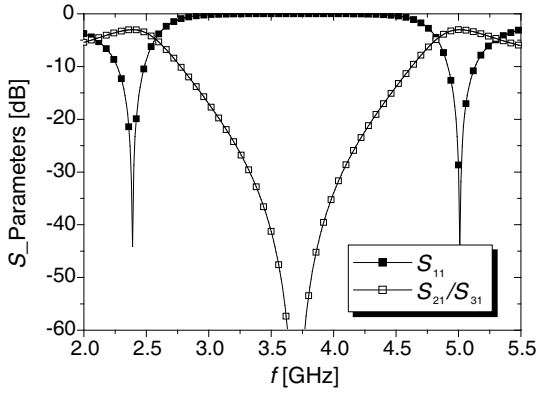

(b)

Figure 6. Schematic-level simulations of proposed dual band baluns for (a) GSM system, and (b) IEEE 802.11 standard.

Table 1. Calculated stub impedance of proposed balun.

f_1 (MHz)	f_2 (MHz)	n	Z_s	Z_{oe}	Z_{oo}	$\Theta_c(@f_1)$
900	1800	1	30	142	26	60°
850	1900	1	30	140	21	55.64°
900	1900	1	30	135	25	58.06°
2400	5000	1	30	137	25	58.38°

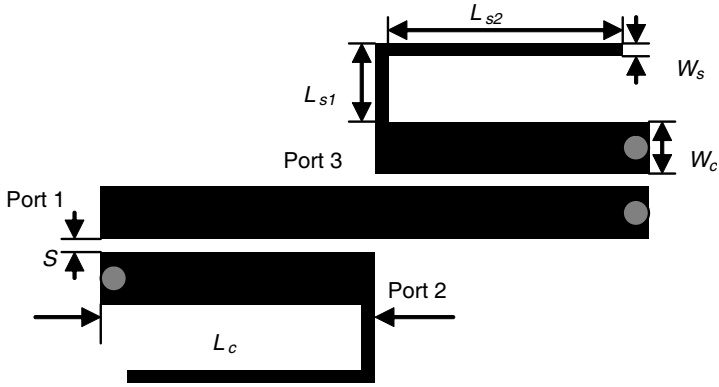

Figure 7. Layout of the proposed dual-band balun. $W_c = 1.78\,\text{mm}$, $W_s = 0.7\,\text{mm}$, $L_c = 20\,\text{mm}$, $L_{s1} = 3.8\,\text{mm}$, $L_{s2} = 14\,\text{mm}$.

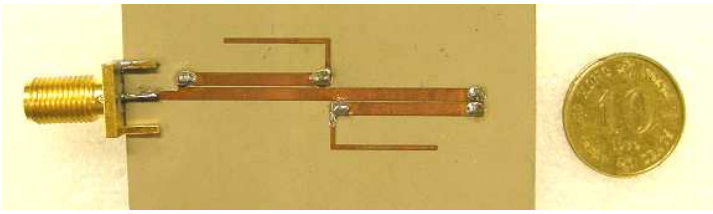

Figure 8. Experimental prototype for proposed balun.

be realized by symmetrical lines such as stripline using multilayer substrate technologies. For microstrip realization, however, special attention is required due to its nature of unequal even and odd mode phase velocities. This undesired property could degrade the performance of the fabricated dual-band balun.

Figure 7 shows a physical layout of proposed dual-band balun. An experimental prototype fabricated on Duroid RO3210 printed circuit board is shown in Fig. 8.

According to the design procedures described above, a set of even-odd mode impedances associated with stub impedances were calculated for a dual-band balun working at 0.9 GHz and 2 GHz. Both coupled-line section and shunted stub have an electric length of 90° at 1.45 GHz, which is the middle frequency of the two operation bands.

Figure 9 shows the measured and full-wave simulated amplitude responses of the fabricated dual-band balun. The overall measured result shows a good agreement with the simulated one. The measured S_{21} and S_{31} are $-2.85/-4.53\,\text{dB}$ at 0.9 GHz, and $-3.97/-3.7\,\text{dB}$

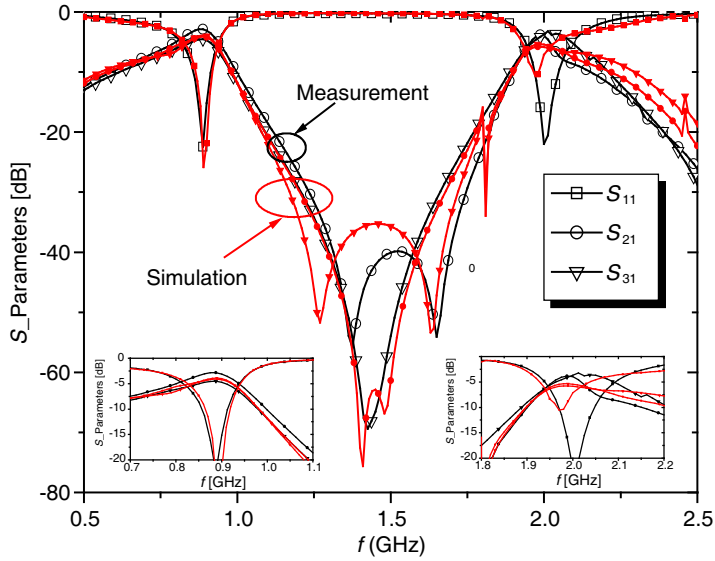

Figure 9. Comparison between simulated and measured results for the proposed dual-band balun.

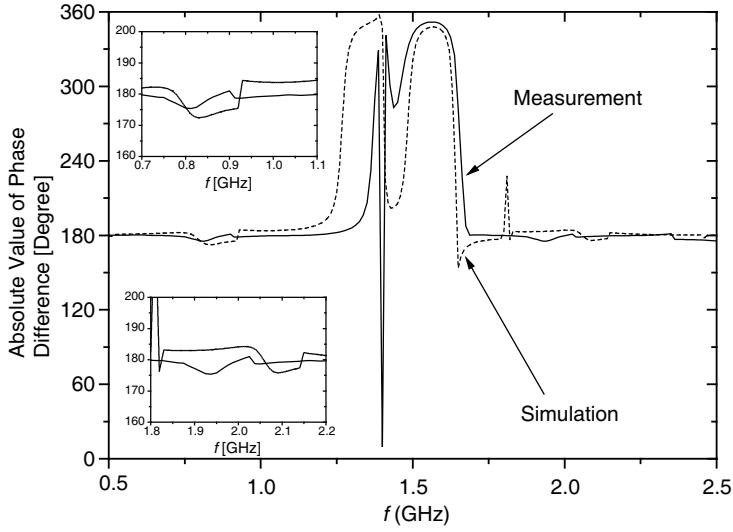

Figure 10. Simulated and measured phase different between the two output ports for the proposed dual-band balun.

at 2 GHz, respectively. According to the measurement, the balun has 32.3% fractional bandwidth at 0.9 GHz and 15.5% fractional bandwidth at 2 GHz. The mismatch in the measurement data is introduced by our measurement setup (e.g., coaxial cables are used to feed port 2 and port 3 from the backside, which introduce additional losses/mismatches). Fig. 10 shows the phase characteristic. In two operation bands, the phase differences are within the range of $180° \pm 2°$, verifying the desired balun operation.

Finally, it is worth to point out that the proposed dual-band balun can be easily redesigned to support other working frequencies with different frequency ratios, although they have higher loss (as shown in Fig. 9) and narrower bandwidth compared with conventional single-band designs. The narrower bandwidth is due to the additional shunted stubs. The higher loss is probably due to the additional cables we used to measure the 50–250 Ω system as shown in Fig. 9.

5. CONCLUSION

A dual-band balun with shunted stubs based on short-ended structure has been presented in this paper. Detailed theoretical calculations of this proposed balun is included. To verify the design concept, an experimental prototype has been fabricated and measured. The measurement results match with the simulations. The proposed dual-band balun features compact size and high design flexibility. It can be easily scaled for other working frequencies. In the future, more flexibility of proposed baluns will be introduced by adjusting the location of the shunted stubs.

REFERENCES

1. Bawer, R. and J. J. Wolfe, "A printed-circuit balun for use with spiralantennas," *IRE Trans. Microw. Theory Tech.*, Vol. 8, 319–325, May 1960.
2. Hallfold, R., "A designer's guide to planar mixer baluns," *Microwaves*, Vol. 18, 52–57, December 1979.
3. Bassett, R., "Three balun designs for push-pull amplifiers," *Microwaves*, Vol. 19, 47–52, July 1980.
4. Ang, K. S. and Y. C. Leong, "Converting baluns into broad-band impedance-transforming 180 hybrids," *IEEE Trans. Microw. Theory Tech.*, Vol. 50, 1190–1195, August 2002.
5. Rajashekharaiah, M., P. Upadhyaya, and H. Deukhyoun, "A compact 5.6 GHz low noise amplifier with new on-chip gain

controllable active balun," *IEEE Workshop on Microelectronics and Electron Devices*, 131–132, 2004.

6. Yoon, Y. J., Y. Lu, R. C. Frye, M. Y. Lau, P. R. Smith, L. Ahlquist, and D. P. Kossives, "Design and characterization of multiplayer spiral transmission-line baluns," *IEEE Trans. Microw. Theory Tech.*, Vol. 47, 1841–1847, September 1999.
7. Kraus, J. D. and R. J. Marhefka, *Antennas for All Application*, 3rd edition, Chapter 23, McGraw-Hill, 2002.
8. Cho, C. and K. C. Gupta, "A new design procedure for single-layer and two-layer three-line baluns," *IEEE Trans. Microw. Theory Tech.*, Vol. 46, 2514–2519, December 1998.
9. Marchand, N., "Transmission-line conversion transformers," *Electronics*, Vol. 17, 142–146, December 1944.
10. Fathelbab, W. M. amd M. B. Steer, "New classes of miniaturized planar Marchand baluns," *IEEE Trans. Microw. Theory Tech.*, Vol. 52, No. 4, 1211–1220, April 2005.
11. Kuman, B. P. and G. R. Branner, "Optimized design of unique miniaturized planar baluns for wireless applications," *IEEE Microw. Wireless Compon. Lett.*, Vol. 13, No. 2, 134–136, February 2003.
12. Lin, C.-M., C.-C. Su, S.-H. Hung, and Y.-H. Wang, "A compact balun based on microstrip EBG cell and interdigital capacitor," *Progress In Electromagnetics Research Letters*, Vol. 12, 111–118, 2009.
13. Yeh, Z.-Y. and Y.-C. Chiang, "A miniature CPW balun constructed with length-reduced 3 dB couples and a short redundant transmission line," *Progress In Electromagnetics Research*, Vol. 117, 195–208, 2011.
14. Jafari, E., F. Hojatkashani, and R. Rezaiesarlak, "A wideband compact planar balun for UHF DTV applications," *Journal of Electromagnetic Waves and Applications*, Vol. 23, Nos. 14–15, 2047–2053, 2009.
15. Basraoui, M. and S. N. Prasad, "Wideband, planar, log-periodic balun," *IEEE MTT-S Int. Microwave Symp. Dig.*, Vol. 2, 785–788, June 1998.
16. Zhang, Z. Y., Y. X. Guo, S. H. Son, H. J. Lee, Y. J. Song, Y. W. Jeong, H. S. Park, and D. Ahn, "Design method of a dual band balun and divider," *IEEE MTT-S Int. Microwave Symp. Dig.*, 1177–1180, June 2002.
17. Guo, Y., Z. Y. Zhang, L. C. Ong, and M. Y. W. Chia, "A novel LTCC miniaturized dual band balun," *IEEE Microw. Wireless*

Compon. Lett., Vol. 16, No. 3, 143–145, March 2006.

18. Yeung, L. K. and K. L. Wu, "A dual-band coupled-line balun filter," *IEEE Trans. Microw. Theory Tech.*, Vol. 55, No. 11, 2406–2411, November 2007.
19. Fathelbab, W. M., "Dual-band marchand baluns," *IEEE International Microwave Symposium (IMS'08)*, 679–682, June 2008.
20. Zhang, H., Y. Peng, and X. Hao, "A tapped stepped-impedance balun with dual-band operations," *IEEE Antennas and Wireless Propagation Lett.*, Vol. 7, 119–122, 2008.
21. Zhang, H. and X. Hao, "A dual-band dipole antenna with integrated-balun," *IEEE Trans. on Antennas and Propagation*, Vol. 57, No. 3, 786–789, March 2009.
22. Leong, Y. C., K. S. Ang, and C. H. Lee, "A derivation of a class of 3-port baluns from symmetrical 4-port networks," *IEEE MTT-S Int. Microwave Symp. Dig.*, June 2002.
23. Ang, K. S., Y. C. Leong, and C. H. Lee, "Analysis and design of miniaturized lumped-distributed impedance transforming baluns," *IEEE Trans. Microw. Theory Tech.*, Vol. 51, No. 3, 1009–1017, March 2003.
24. Matthaei, G., L. Young, and E. M. T. Jones, *Microwave Filters, Impedance-Matching Networks, and Coupling Structures*, Artech House, 1980.